Inverse Lax-Wendroff Procedure for Numerical Boundary Conditions

Chi-Wang Shu

Division of Applied Mathematics

Brown University

Joint work with Shanqin Chen, Shengrong Ding, Jinwei Fang, Ling Huang, Fengyan Li, Tingting Li, Jianfang Lu, Jianguo Ning, Sirui Tan, Francois Vilar, Cheng Wang, Tao Xiong, Mengping Zhang, Yong-Tao Zhang and Hongkai Zhao

Outline

- Introduction
- Steady state Hamilton-Jacobi equations
- Time dependent hyperbolic equations
- Compressible inviscid flows involving complex moving geometries
- Convection-diffusion equations
- Conclusions and future work

Introduction

For finite difference schemes approximating PDEs, there are two major difficulties associated with numerical boundary conditions:

- High order finite difference schemes involve a wide stencil, hence there are several points near the boundary (either as ghost points outside the computational domain or as the first few points inside the computational domain near the boundary) which need different treatment.

For example, if we have the following scheme

$$u_j^{n+1} = au_{j-2}^n + bu_{j-1}^n + cu_j^n + du_{j+1}^n$$

with suitably chosen constants a, b, c and d (which depend on $\lambda = \frac{\Delta t}{\Delta x}$), approximating the PDE

$$u_t + u_x = 0,$$

$$u(x,0) = f(x), \qquad u(0,t) = g(t)$$

to third order accuracy, then either a ghost point u_{-1}^n is needed, or the scheme cannot be used to compute u_1^{n+1}.

- The boundary of the computational domain may not coincide with grid points.

  For example, in 1D, we may have the physical boundary $x = 0$ located anywhere between two grid points. While this seems artificial, it is unavoidable for a moving boundary computed on a fixed grid.

  This difficulty is more profound in 2D (complicated geometry computed on Cartesian meshes).

  One of the major difficulties is the small cell near the boundary and the resulting small time step required for stability (the so-called “cut-cell problem”.

Previous work on numerical boundary conditions:

- h-box method of Berger, Helzel and LeVeque (SINUM 2003): suitable flux computation based on cells of size h. This method can overcome the difficulty of small time step for stability, but is somewhat complicated in 2D and for high order accuracy.

- Reflecting or symmetry boundary conditions for ghost points: suitable for solid walls or symmetry lines which are straight lines but lead to large errors for curved walls not aligned with meshes.

- Extrapolation to obtain ghost point values (Kreiss et al SINUM 2002, 2004; SISC 2006; Sjögreen and Petersson CiCP 2007). A GKS stability analysis must be performed to assess its stability. Second order is fine but higher order is more complicated to analyze. It is not stable if the physical boundary is too close to a grid point.
- Converting spatial derivative near the boundary to temporal derivatives (Goldberg and Tadmor, Math Comp 1978, 1981 for one-dimensional linear hyperbolic initial-boundary value problems).
- Compatible boundary conditions for boundaries and interfaces (Henshaw, Kreiss and Reyna, Computers & Fluids 1994; Henshaw, SISC 2006; Henshaw and Chand, JCP 2009).

Review on the traditional Lax-Wendroff procedure for solving, e.g.

$$u_t + u_x = 0$$

- Taylor expansion in time

$$u_j^{n+1} = u_j + (u_t)_j \Delta t + \frac{1}{2}(u_{tt})_j \Delta t^2 + ...$$

- Replace the time derivatives by spatial derivatives by repeatedly using the PDE:

$$(u_t)_j = -(u_x)_j$$

$$(u_{tt})_j = -((u_x)_t)_j = -((u_t)_x)_j = (u_{xx})_j$$

...

- Approximate the spatial derivatives by finite differences of suitable order of accuracy.

We now look at the basic idea of the inverse Lax-Wendroff procedure, by switching the roles of x and t in the traditional Lax-Wendroff procedure. Suppose we are solving

$$u_t + u_x = 0, \qquad u(0,t) = g(t)$$

and suppose the boundary $x = 0$ is of distance $a\Delta x$ from x_1 (with a constant a), the inverse Lax-Wendroff procedure to determine u_1 is as follows:

- Taylor expansion in space

$$u_1 = u(0,t) + u_x(0,t)a\Delta x + \frac{1}{2}u_{xx}(0,t)(a\Delta x)^2 + ...$$

- Replace the spatial derivatives by time derivatives by repeatedly using the PDE:

$$u_x = -u_t; \qquad u_x(0,t) = -u_t(0,t) = -g'(t)$$

$$u_{xx} = (-u_t)_x = -(u_x)_t = u_{tt};$$

$$u_{xx}(0,t) = u_{tt}(0,t) = g''(t)$$

...

- Compute $g'(t)$, $g''(t)$, etc. either analytically or by finite difference.

Steady state Hamilton-Jacobi equations

We are interested in the steady state solution of the Hamilton-Jacobi equation

$$H(\phi_x, \phi_y) = f(x, y) \tag{1}$$

together with suitable boundary conditions.

We can use Runge-Kutta or other methods to march in time for the time dependent PDE

$$\phi_t + H(\phi_x, \phi_y) = f(x, y) \tag{2}$$

until steady state is reached, but that is rather slow.

One class of effective numerical methods is the fast sweeping method (Boué and Dupuis, SINUM 1999; Zhao, Math Comp 2005). For high order finite difference fast sweeping methods (Zhang, Zhao and Qian, JSC 2006), the first few points near an inflow boundary are usually prescribed to be the exact solution. This is not practical for problems with unknown exact solutions.

To fix the ideas, let us assume that the left boundary

$$\Gamma = \{(x, y) : x = 0,\ 0 \leq y \leq 1\} \tag{3}$$

of the computational domain $[0, 1]^2$ is the inflow boundary, on which the solution is given as

$$\phi(0, y) = g(y), \qquad 0 \leq y \leq 1.$$

We would like to obtain a high order approximation to the solution value $\phi_{i,j} \approx \phi(x_i, y_j)$ for $i = 1, 2$ and a fixed j, which corresponds to a point (x_i, y_j) near the inflow boundary which cannot be computed by the high order WENO scheme. A simple Taylor expansion gives, for $i = 1, 2$,

$$\phi(x_i, y_j) = \phi(0, y_j) + ih\,\phi_x(0, y_j) + \frac{(ih)^2}{2}\phi_{xx}(0, y_j) + O(h^3)$$

hence our desired approximation for the third order WENO scheme is

$$\phi_{i,j} = \phi(0, y_j) + ih\,\phi_x(0, y_j) + \frac{(ih)^2}{2}\phi_{xx}(0, y_j).$$

We already have $\phi(0, y_j) = g(y_j)$. The PDE (1), evaluated at the point $(0, y_j)$, becomes

$$H(\phi_x(0, y_j), g'(y_j)) = f(0, y_j) \tag{4}$$

in which the only unknown quantity is $\phi_x(0, y_j)$. Solving this (usually nonlinear) equation should give us $\phi_x(0, y_j)$.

To obtain $\phi_{xx}(0, y_j)$, we first take the derivative with respect to y on the original PDE (1), and then evaluate it at the the point $(0, y_j)$, which yields

$$\partial_u H(\phi_x(0, y_j), g'(y_j))\phi_{xy}(0, y_j) + \partial_v H(\phi_x(0, y_j), g'(y_j))g''(y_j) = f_y(0, y_j). \tag{5}$$

In this equation the only unknown quantity is $\phi_{xy}(0, y_j)$, hence we obtain easily its value.

We then take the derivative with respect to x on the original PDE (1), and evaluate it at the the point $(0, y_j)$ to obtain

$$\partial_u H(\phi_x(0, y_j), g'(y_j))\phi_{xx}(0, y_j) + \partial_v H(\phi_x(0, y_j), g'(y_j))\phi_{xy}(0, y_j) = f_x(0, y_j),$$

This time, the only unknown quantity is $\phi_{xx}(0, y_j)$, which we can obtain readily from this equality.

It is clear that this procedure can be carried out to any desired order of accuracy. Also, the inflow boundary Γ in (3) can be any piece of a smooth curve and does not need to be aligned with the mesh points: we only need to change the x and y partial derivatives to normal and tangential derivatives with respect to Γ. However, for this approach to work, Γ can not consist of a single point.

Example 1. We solve the Eikonal equation with $f(x,y) = 1$. The computational domain is $[-1,1]^2$, and the inflow boundary Γ is the unit circle of center (0,0) and radius 0.5, that is

$$\Gamma = \left\{ (x,y) : \ x^2 + y^2 = \frac{1}{4} \right\}.$$

The boundary condition $\phi(x,y) = 0$ is prescribed on Γ. The exact solution for this problem is the distance function to the circle Γ. This exact solution has a singularity at the center of the circle to which the characteristics converge, hence we exclude the box $[-0.15, 0.15]^2$ when measuring the errors. Notice that for this example, the domain boundary Γ is *not* aligned with the Cartesian mesh. We again use third order WENO scheme with the fast sweeping method.

Table 1: Example 1. Lax-Wendroff type procedure for the inflow boundary. N is the number of mesh points in each direction. The errors are measured in the computational domain but outside the box $[-0.15, 0.15]^2$.

N	L^1 error	order	L^∞	order	iteration number
80	0.573E-05		0.129E-03		25
160	0.122E-05	2.23	0.407E-05	4.98	32
320	0.191E-06	2.68	0.122E-05	1.74	46
640	0.246E-07	2.95	0.161E-06	2.92	62

References:

[1] L. Huang, C.-W. Shu and M. Zhang, *Numerical boundary conditions for the fast sweeping high order WENO methods for solving the Eikonal equation*, Journal of Computational Mathematics, v26 (2008), pp.336-346.

[2] T. Xiong, M. Zhang, Y.-T. Zhang and C.-W. Shu, *Fifth order fast sweeping WENO scheme for static Hamilton-Jacobi equations with accurate boundary treatment*, Journal of Scientific Computing, v45 (2010), pp.514-536.

[3] Y.-T. Zhang, S. Chen, F. Li, H. Zhao and C.-W. Shu, *Uniformly accurate discontinuous Galerkin fast sweeping methods for Eikonal equations*, SIAM Journal on Scientific Computing, v33 (2011), pp.1873-1896.

Time dependent hyperbolic equations

The same idea we mentioned in the introduction can be used to strongly hyperbolic conservation laws for $\boldsymbol{U} = \boldsymbol{U}(x, y, t) \in \mathbb{R}^2$

$$\begin{cases} \boldsymbol{U}_t + \boldsymbol{F}(\boldsymbol{U})_x + \boldsymbol{G}(\boldsymbol{U})_y = 0 & (x, y) \in \Omega, \quad t > 0, \\ \boldsymbol{U}(x, y, 0) = \boldsymbol{U}_0(x, y) & (x, y) \in \bar{\Omega}, \end{cases} \tag{6}$$

on a bounded domain Ω with appropriate boundary conditions prescribed on $\partial\Omega$ at time t. We assume Ω is covered by a uniform Cartesian mesh $\Omega_h = \{(x_i, y_j) : 0 \leqslant i \leqslant N_x, 0 \leqslant j \leqslant N_y\}$ with mesh size $\Delta x = \Delta y$.

One difficulty of this procedure, especially for nonlinear systems in multiple-dimensions, is that the algebra becomes very heavy for higher order derivatives.

In (Tan, Wang, Shu and Ning, JCP 2012), a simplified version of this inverse Lax-Wendroff procedure is adopted. This procedure is used only to compute the first spatial derivative u_x, subsequent derivatives u_{xx} etc. are obtained by standard extrapolation with suitable order of accuracy.

The computational examples in (Tan, Wang, Shu and Ning, JCP 2012) are for physical boundaries aligned with the mesh points. For such cases and for fifth order WENO schemes, this simplified inverse Lax-Wendroff procedure works very well with stable results in very demanding detonation problems.

In (Vilar and Shu, M^2AN 2015), we perform a rigorous stability analysis using the GKS (Gustafsson, Kreiss and Sundström) theory, using the class of central compact schemes in (Liu, Zhang, Zhang and Shu, JCP 2013) as examples. This analysis is also performed for upwind-biased finite difference schemes (prototypes of WENO schemes with linear weights) in (Li, Shu and Zhang, JCAM 2016).

This analysis gives explicit guidance on how many terms of u_x, u_{xx}, ... are required to be treated by the inverse Lax-Wendroff procedure in order to maintain stability (for the fully discrete case, under the same CFL number as in the periodic case) for arbitrary location of the boundary in relation to the nearest grid point.

Two different techniques, one based on normal mode GKS analysis and the other based on eigenstructure analysis of amplification matrices, are performed, and are shown to lead to identical conclusions regarding stability when both work.

Scheme	Required leading terms
CCS-T4	3
CCS-T6	3
CCS-T8	5
CCS-T10	8
CCS-T12	9

Table 2: Minimum number of leading terms with ILW procedure required by the different RK3-CCS-tridiagonal schemes to remain stable under the same CFL as that for periodic boundary conditions.

Scheme	$(k_d)_{\min}$
Third order scheme	2
Fifth order scheme	3
Seventh order scheme	4
Ninth order scheme	6
Eleventh order scheme	8
Thirteenth order scheme	10

Table 3: Minimum number of leading terms with ILW procedure required by the different upwind-biased schemes with RK3 time discretization to remain stable under the same CFL as that for periodic boundary conditions.

At the outflow boundary, extrapolation of appropriate order is used. Either a regular or a WENO type extrapolation is appropriate depending on whether the outflow solution is smooth or contains shocks.

For the outflow boundary condition, we can show that the scheme with the extrapolation is stable for all order s.

We remark that the time step restriction of solving the system of ODEs with our boundary treatment is not more severe than the pure initial value problem. The standard CFL conditions determined by the interior schemes are used in the numerical examples.

When solving nonlinear conservation laws

$$u_t + f(u)_x = 0,$$

if the boundary condition is given at the left boundary $x = 0$

$$u(0, t) = g(t),$$

then the inverse Lax-Wendroff procedure is to obtain $u_x(0, t)$ through the PDE:

$$u_x(0, t) = -\frac{u_t(0, t)}{f'(u(0, t))} = -\frac{g'(t)}{f'(g(t))}.$$

This works well if $f'(g(t)) > 0$ (to justify giving a boundary condition at the left boundary $x = 0$), but it causes problems if $f'(g(t))$ is very close to zero or is zero (close to or at the sonic points).

In Lu, Shu, Tan and Zhang, JCP submitted, an alternative procedure is introduced to obtain the values of $f(u)$ (instead of u) at the ghost points by the inverse Lax-Wendroff procedure. Then, we would need $f(u)_x$ at $x = 0$, which can be readily obtained as

$$(f(u)_x)|_{(0,t)} = -u_t(0,t) = -g'(t).$$

The remaining higher spatial derivatives of $f(u)$ are obtained by extrapolation. This alternative procedure works well at or near sonic points, allowing a smooth transition from inflow to outflow boundaries, especially for systems.

An important issue for conservation laws is numerical conservation. While this is straightforward for finite volume schemes, the very definition of conservation is not clear for finite difference schemes.

For a conservative finite difference scheme

$$u_j^{n+1} = u_j^n - \frac{\Delta t}{\Delta x}\left(\hat{f}_{j+\frac{1}{2}} - \hat{f}_{j-\frac{1}{2}}\right) \tag{7}$$

where u_j is an approximation to the point value of the solution $u(x,t)$, the locally conserved variable appears to be $u_j \Delta x$ (in the sense that its change over time is purely due to the net inflow and outflow through the cell boundaries $x = x_{j-\frac{1}{2}}$ and $x = x_{j+\frac{1}{2}}$), and the conserved total "mass" appears to be

$$\tilde{S} = \sum_{j=0}^{N} u_j \Delta x, \tag{8}$$

in the sense that

$$\tilde{S}^{n+1} = \tilde{S}^n - \Delta t \left(\hat{f}_{N+\frac{1}{2}} - \hat{f}_{-\frac{1}{2}} \right)$$

and, with periodic or compactly supported boundary conditions, $\hat{f}_{N+\frac{1}{2}} = \hat{f}_{-\frac{1}{2}}$ and we have total "mass" conservation

$$\tilde{S}^{n+1} = \tilde{S}^n.$$

In fact, even though the local "mass"

$$u_j \Delta x = \bar{u}_j \Delta x + O(\Delta x^3)$$

is only a third order approximation to the true local mass $\bar{u}_j \Delta x$ in smooth regions, the total "mass" $\tilde{S}$, as defined in (8), is equal to the true total

mass S

$$S = \int_a^b u(x,t)dx, \tag{9}$$

for any N-th degree trigonometric polynomial (assuming N is even for convenience)

$$u(x) = \sum_{k=-N/2}^{N/2} a_k e^{ikx}. \tag{10}$$

That is,

$$\tilde{S} = \sum_{j=0}^{N} u_j \Delta x = \sum_{j=0}^{N} \bar{u}_j \Delta x = S$$

if the point values u_j and the cell averages $\bar{u}_j$ are both from an N-th degree trigonometric polynomial (10). Therefore, a conservative finite difference scheme (7) conserves the total "mass" $\tilde{S}$ as defined in (8),

which is a spectrally accurate approximation to the true total mass S as defined in (9), for any smooth periodic or compactly supported solutions.

However, if the solution is not periodic or compactly supported, then we only have

$$\tilde{S} = \sum_{j=0}^{N} u_j \Delta x = \sum_{j=0}^{N} \bar{u}_j \Delta x + O(\Delta x^2) = S + O(\Delta x^2). \qquad (11)$$

That is, the total "mass" $\tilde{S}$, as defined in (8), is only a second order approximation to the true total mass S for non-periodic functions. Therefore, if a finite difference scheme conserves the total "mass" $\tilde{S}$ (subject to net inflow and outflow at the domain boundaries), it can only be second order accurate.

This problem exists already for regular finite difference schemes, but is compounded by the inverse Lax-Wendroff procedure at the numerical boundaries.

In Ding, Shu and Zhang, JCP 2020, we obtained conservative finite difference schemes using the inverse Lax-Wendroff procedure, with the following ingredients:

- Using the numerical quadrature formula

$$\int_0^{\infty} h(x)dx = \Delta x \sum_{j=0}^{+\infty} \omega_j h(x_j) + O\left((\Delta x)^{\nu}\right), \qquad (12)$$

where the weights ω_j depend on ν, but $\omega_j = 1$ for $j \geq \nu$, we define the numerical total mass consistent with high order accuracy to the

true total mass as

$$\tilde{S} = \sum_{j=0}^{N} \omega_j u_j \Delta x. \tag{13}$$

- We modify the numerical fluxes near the boundary (the modification is local and is a high order accuracy perturbation from the original inverse Lax-Wendroff scheme), so that the resulting scheme is conservative (subject to inflow and outflow) with respect to the numerical total mass (13).
- The conservative inverse Lax-Wendroff scheme works equally well as the original inverse Lax-Wendroff scheme in accuracy and non-oscillatory performance, through extensive numerical tests, and it shows an advantage in shock location resolution for long time simulation.

Example 2. We test the Burgers equation

$$\begin{cases} u_t + \left(\frac{1}{2}u^2\right)_x = 0 & x \in (-1,1), \quad t > 0, \\ u(x,0) = 0.25 + 0.5\sin(\pi x) & x \in [-1,1], \\ u(-1,t) = g(t) & t > 0. \end{cases} \tag{14}$$

Here $g(t) = w(-1,t)$, where $w(x,t)$ is the exact solution of the initial value problem on $(-1,1)$ with periodic boundary conditions. For all t, the left boundary $x = -1$ is an inflow boundary and the right boundary $x = 1$ is an outflow boundary.

Table 4: Errors of the Burgers equation (14). $\Delta x = 2/N$ and $t = 0.3$.

N	L^1 error	order	L^∞ error	order
40	9.11E-05		3.56E-04	
80	3.10E-06	4.88	1.35E-05	4.72
160	1.31E-07	4.57	6.51E-07	4.38
320	3.97E-09	5.05	2.68E-08	4.60
640	1.02E-10	5.29	8.34E-10	5.00
1280	2.86E-12	5.15	2.62E-11	5.00

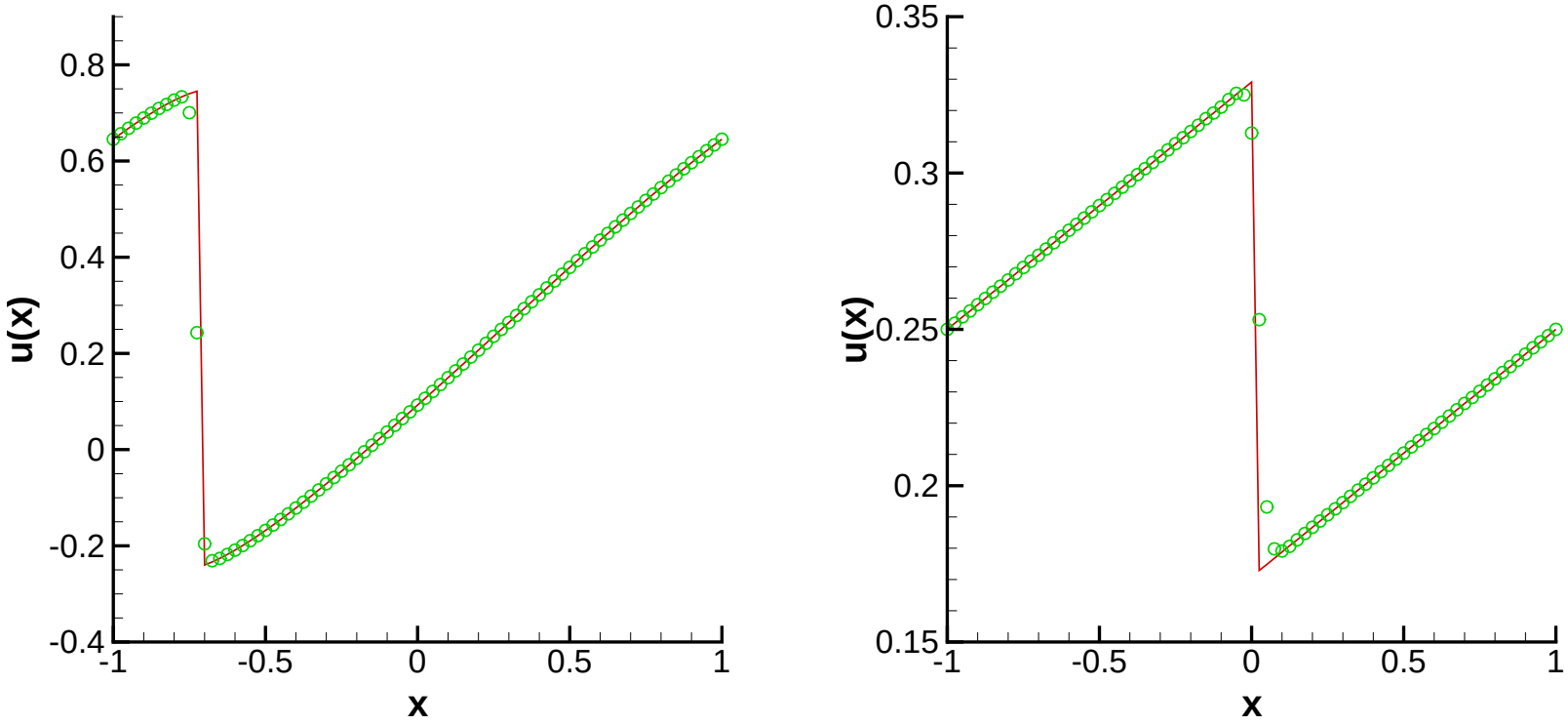

(a) $t = 1.1$ (b) $t = 12$

Figure 1: Burgers equation (14), $\Delta x = 1/40$. Solid line: exact solution; Symbols: numerical solution.

Example 3. Euler equations, blast wave example. We consider the interaction of two blast waves. The initial data are

$$\boldsymbol{U}(x,0) = \begin{cases} \boldsymbol{U}_L & 0 < x < 0.1, \\ \boldsymbol{U}_M & 0.1 < x < 0.9, \\ \boldsymbol{U}_R & 0.9 < x < 1, \end{cases}$$

where $\rho_L = \rho_M = \rho_R = 1$, $u_L = u_M = u_R = 0$, $p_L = 10^3, p_M = 10^{-2}, p_R = 10^2$. There are solid wall boundary conditions at both $x = 0$ and $x = 1$. This problem involves multiple reflections of shocks and rarefactions off the walls. There are also multiple interactions of shocks and rarefactions with each other and with contact discontinuities.

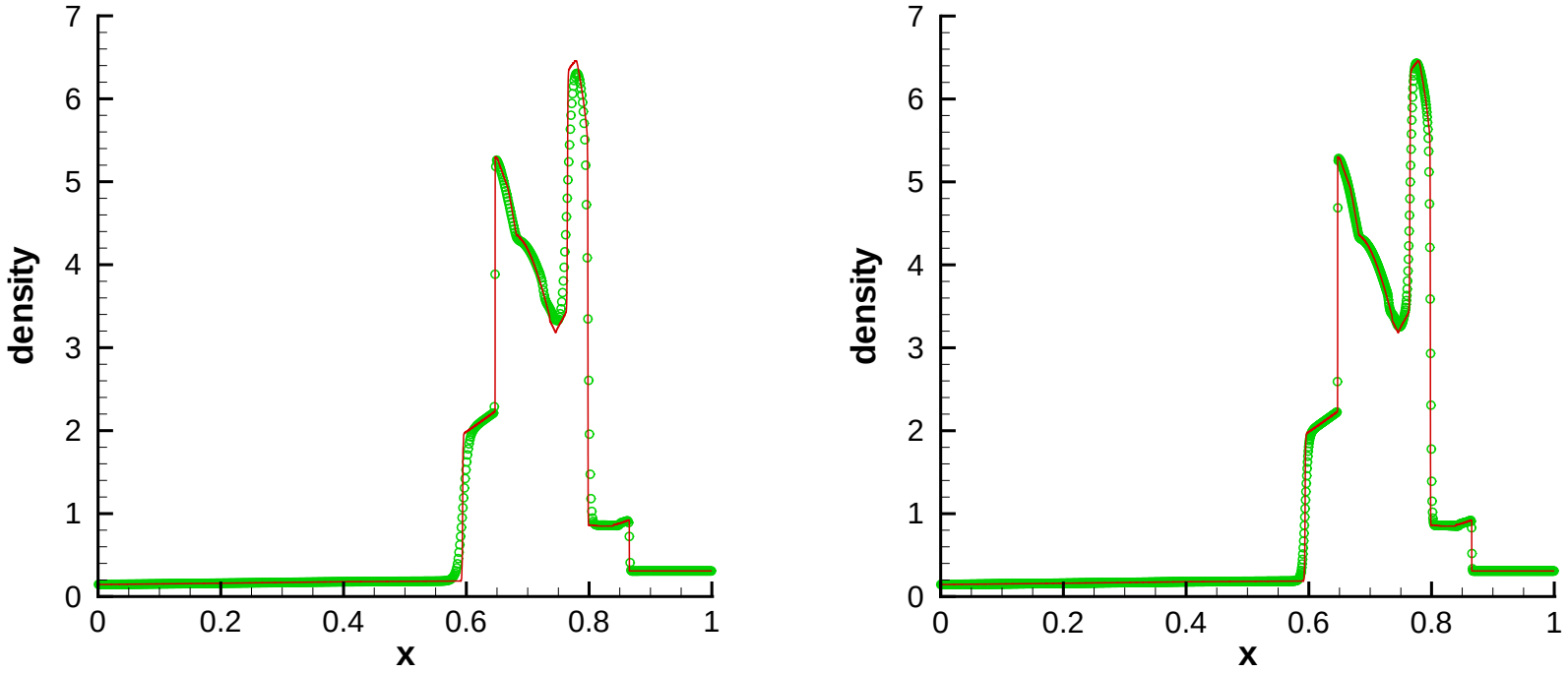

(a) $\Delta x = 1/800$ (b) $\Delta x = 1/1600$

Figure 2: The density profiles of the blast wave problem. Solid lines: reference solution computed by the fifth order WENO scheme with $\Delta x = 1/16000$; Symbols: numerical solutions by our boundary treatment.

To better illustrate the advantage of the conservation method, we give the results for a longer time simulation with a coarser mesh. Figure 3 shows the results of the modified and original SILW methods at $t = 19$ with $N = 800$ grid points.

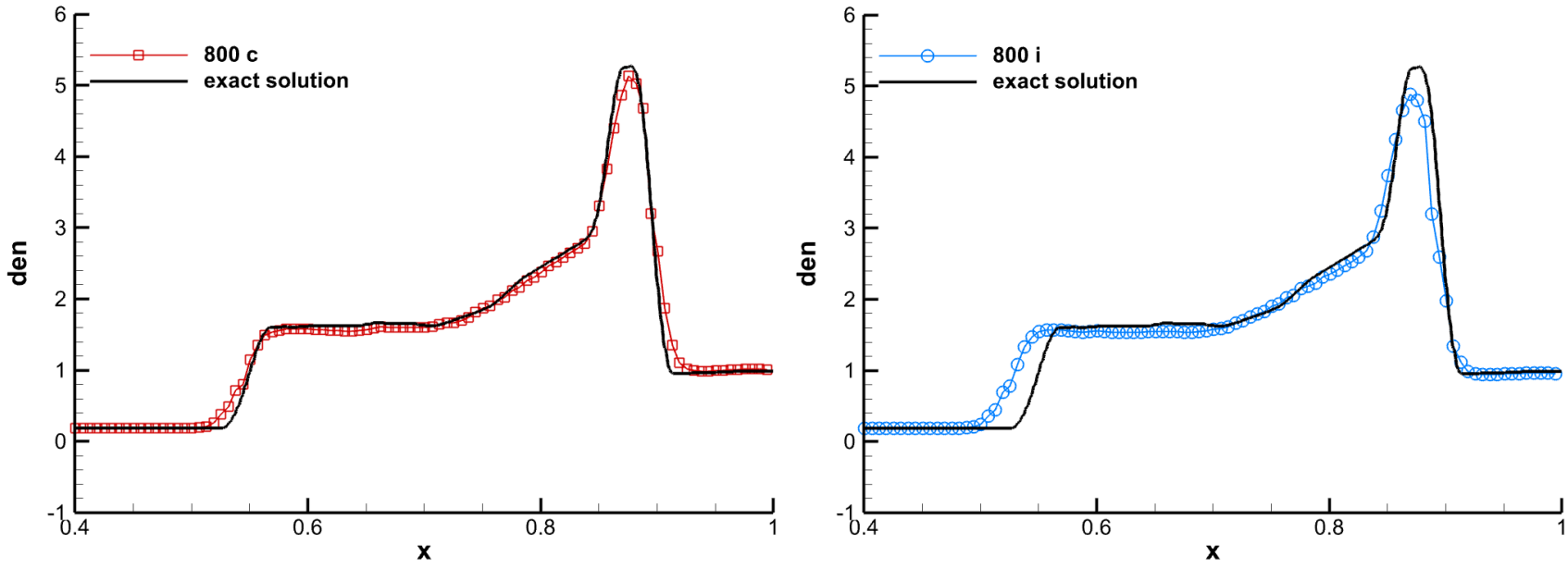

(a) density profile with the modified method (b) density profile with the SILW method

Figure 3: The density profiles of the blast wave problem. $t = 19$. Black solid line: the reference "exact" solution; red solid line with square symbols on the left: numerical solution with the modified method; blue solid line with square symbols on the right: numerical solution with the SILW method.

Example 4. We test the 2D Burgers equation

$$\begin{cases} u_t + \frac{1}{2}\left(u^2\right)_x + \frac{1}{2}\left(u^2\right)_y = 0 & (x,y) \in \Omega, \quad t > 0, \\ u(x,y,0) = 0.75 + 0.5\sin\left[\pi(x+y)\right] & (x,y) \in \bar{\Omega}, \\ u(x,y,t) = g(x,y,t) & (x,y) \in \Gamma, \quad t > 0, \end{cases} \tag{15}$$

where

$$\begin{aligned} \Omega &= (-1,1) \times (-1,1), \\ \Gamma &= \{(x,y) : x = -1 \text{ or } y = -1\}, \end{aligned}$$

or

$$\begin{aligned} \Omega &= \{(x,y) : x^2 + y^2 < 0.5\}, \\ \Gamma &= \{(x,y) : x^2 + y^2 = 0.5 \text{ and } x + y \leqslant 0\}. \end{aligned}$$

Here $g(x, y, t) = w(x, y, t)$, where $w(x, y, t)$ is the exact solution of the initial value problem on $(-1, 1) \times (-1, 1)$ with periodic boundary conditions. Notice that in the second case the domain boundary is not aligned with the Cartesian meshes.

Table 5: Errors of the 2D Burgers equation (15). $\Delta x = 2/N_x, \Delta y = 2/N_y, t = 0.15$.

$N_x = N_y$	on a square				on a disk			
	L^1 error	order	L^∞ error	order	L^1 error	order	L^∞ error	order
40	1.55E-04		9.86E-03		1.10E-04		1.77E-03	
80	1.06E-05	3.87	1.80E-03	2.46	7.24E-06	3.93	4.06E-04	2.12
160	4.93E-07	4.43	2.38E-04	2.91	4.65E-07	3.96	4.77E-05	3.09
320	3.47E-08	3.83	2.83E-05	3.08	3.63E-08	3.68	6.04E-06	2.98
640	2.72E-09	3.67	2.85E-06	3.31	4.10E-09	3.15	9.45E-07	2.68

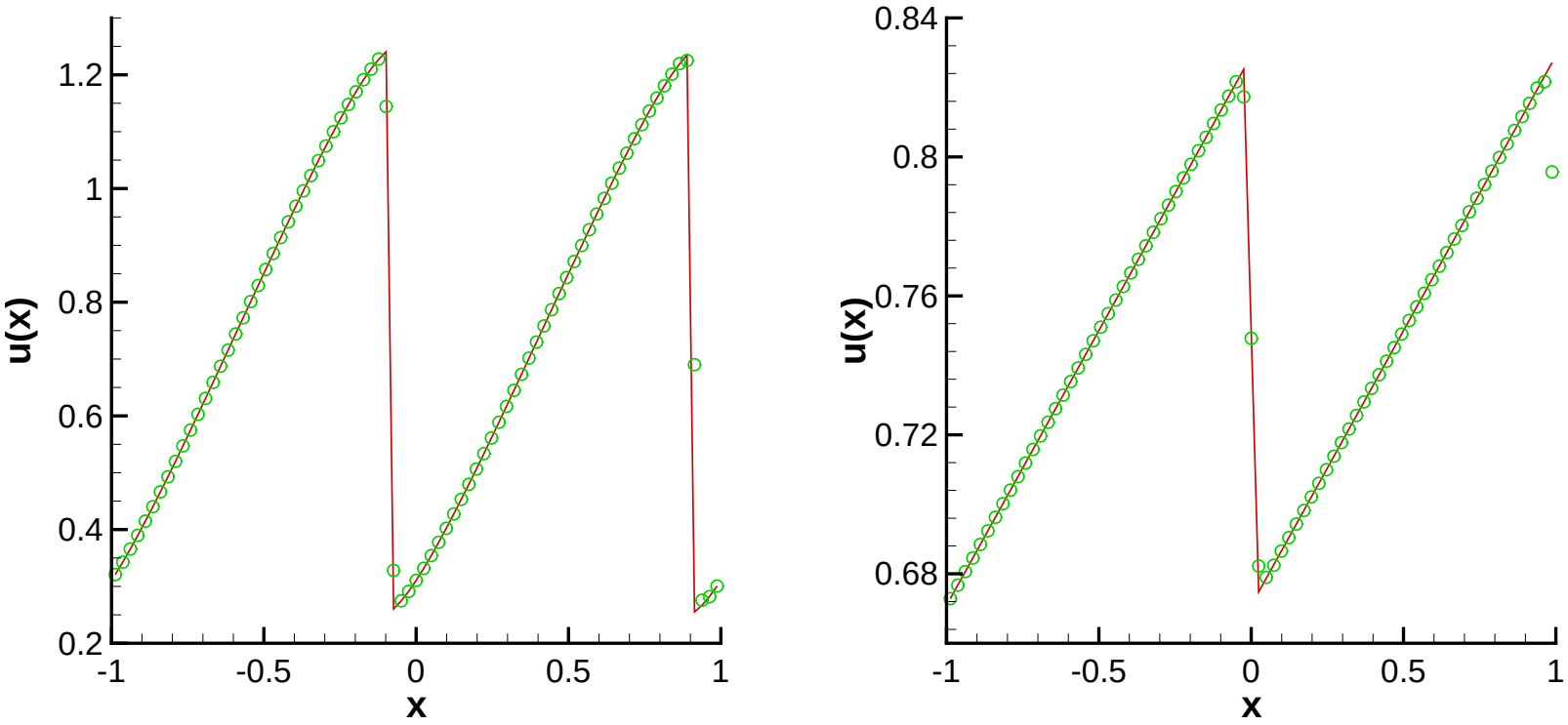

(a) on a square, $t = 0.55$

(b) on a square, $t = 6$

Figure 4: 2D Burgers equation (15). $\Delta x = \Delta y = 1/40$. Cut along the diagonal. Solid line: exact solution; Symbols: numerical solution.

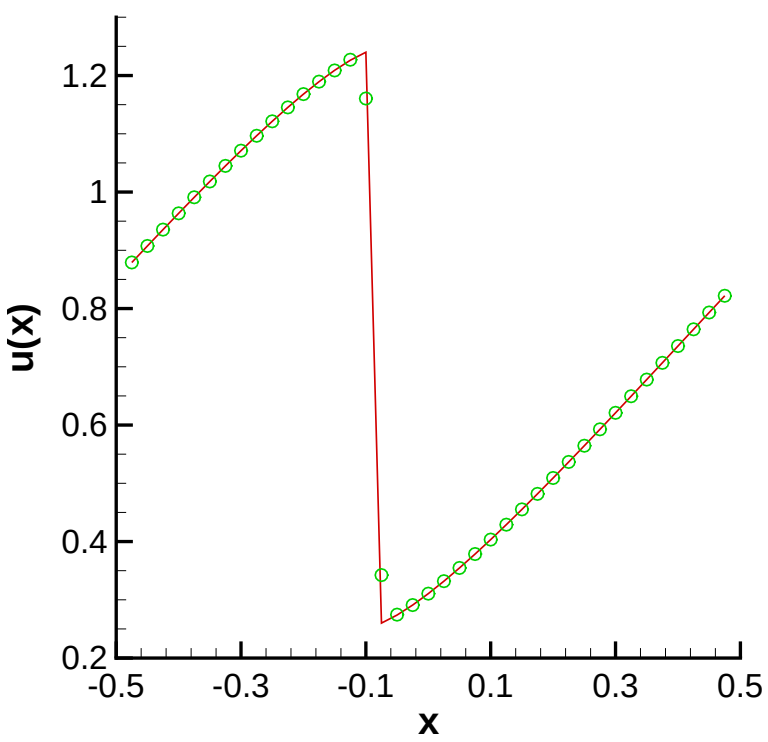

(a) on a disk, $t = 0.55$

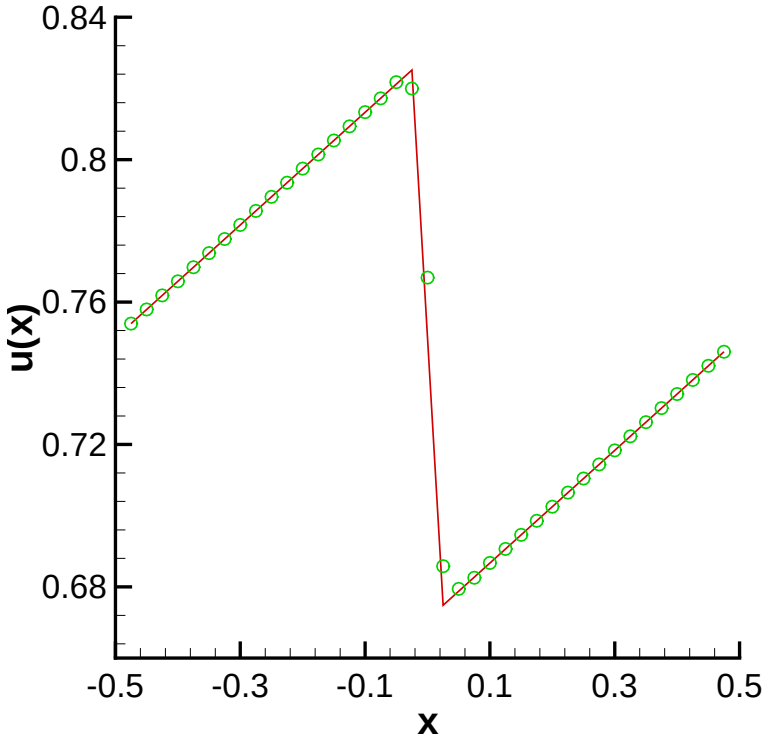

(b) on a disk, $t = 6$

Figure 5: Continued.

Example 5. We are most interested in applying our method to the solid wall boundary conditions $(u, v) \cdot \boldsymbol{n} = 0$, when the wall is not aligned with the grid and can be curved. Our first example of this kind is the double Mach reflection problem. This problem is initialized by sending a horizontally moving shock into a wedge inclined by a 30° angle. In order to impose the solid wall condition by the reflection technique, people usually solve an equivalent problem that puts the solid wall horizontal and puts the shock 60° angle inclined to the wall. Another way to avoid the trouble of imposing boundary conditions is to use a multidomain WENO method. With the use of our method, we are able to solve the original problem with a uniform mesh in a single domain.

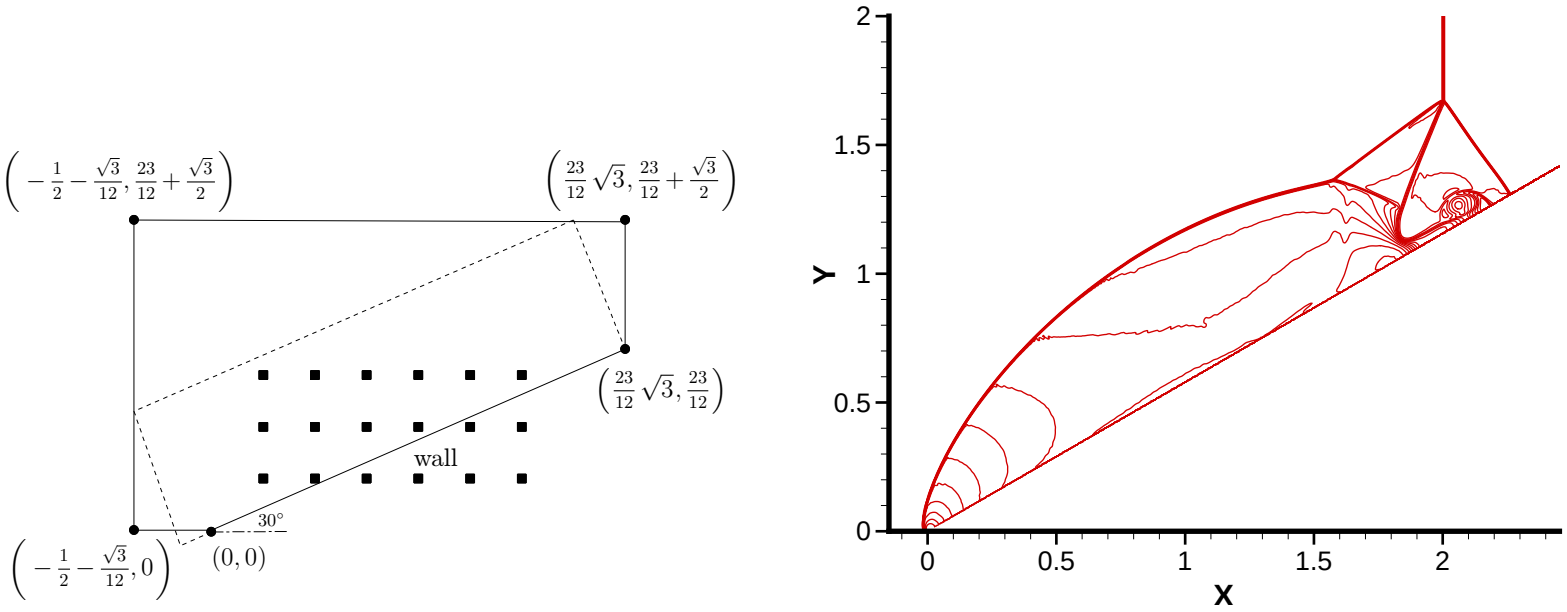

(a) computational domain (b) density contour

Figure 6: Left: The computational domain (solid line). The dashed line indicates the computational domain used in the traditional finite difference solvers. The square points indicate some of the grid points. Right: Density contour of double Mach reflection. $\Delta x = \Delta y = \frac{1}{320}$.

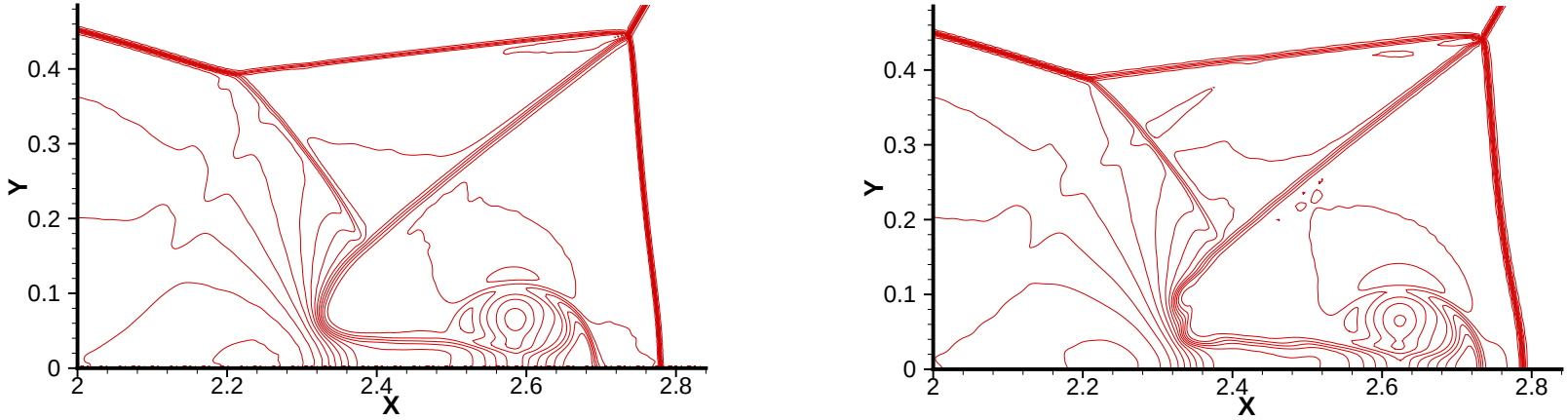

(a) $\Delta x = \Delta y = \frac{1}{320}$, original problem (b) $\Delta x = \Delta y = \frac{\sqrt{3}}{480}$, equivalent problem

Figure 7: Density contours of double Mach reflection, 30 contours from 1.731 to 20.92. Zoomed-in near the double Mach stem. The plots in the left column (our computation with the new boundary condition treatment) are rotated and translated for comparison.

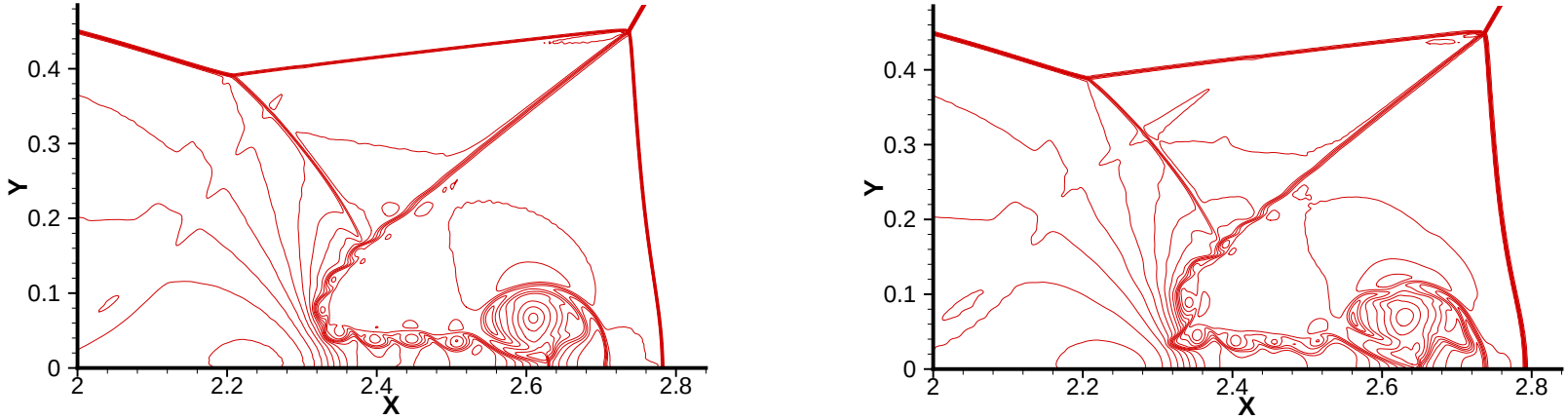

(a) $\Delta x = \Delta y = \frac{1}{640}$, original problem (b) $\Delta x = \Delta y = \frac{\sqrt{3}}{960}$, equivalent problem

Figure 8: Continued

.

Example 6. This example involves a curved wall which is a circular cylinder of unit radius positioned at the origin on a x-y plane. The problem is initialized by a Mach 3 flow moving toward the cylinder from the left. In order to impose the solid wall boundary condition at the surface of the cylinder by the reflection technique, a particular mapping from the unit square to the physical domain is usually used in traditional finite difference methods. Using our method, we are able to solve this problem directly in the physical domain.

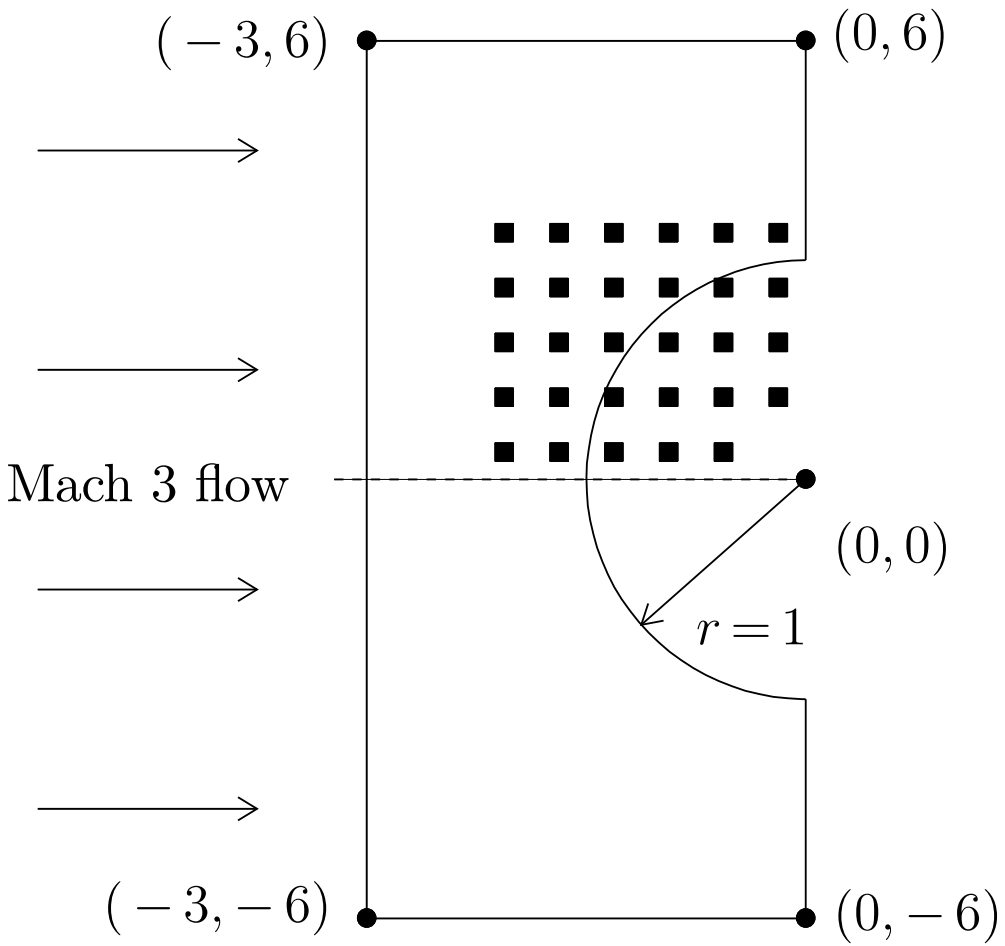

Figure 9: Physical domain of flow past a cylinder. The square points indicate some of the grid points near the cylinder. Illustrative sketch, not to scale.

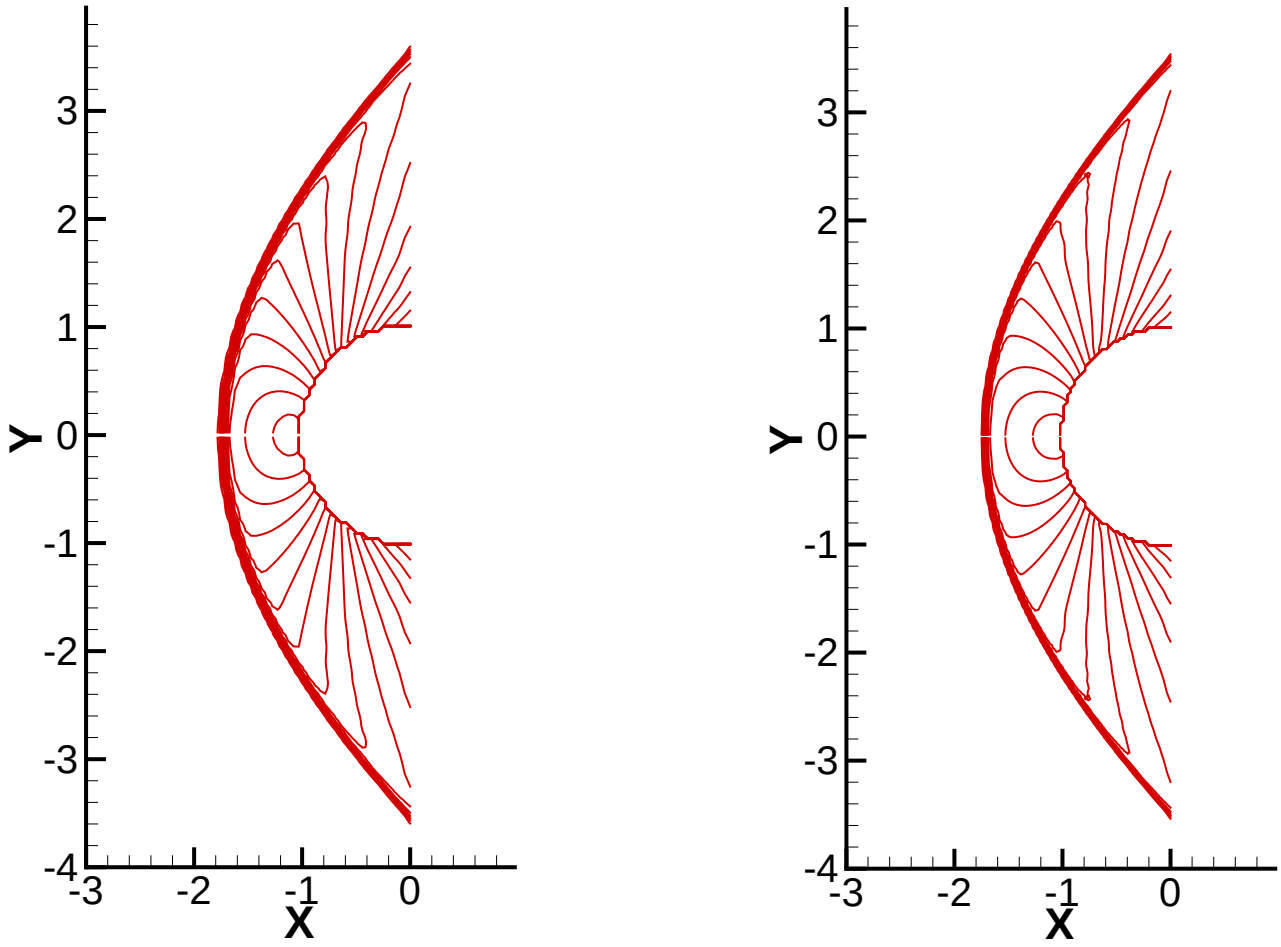

(a) $\Delta x = \Delta y = \frac{1}{20}$ (b) $\Delta x = \Delta y = \frac{1}{40}$

Figure 10: Pressure contour of flow past a cylinder.

Reference:

[4] S. Tan and C.-W. Shu, *Inverse Lax-Wendroff procedure for numerical boundary conditions of conservation laws*, Journal of Computational Physics, v229 (2010), pp.8144-8166.

[5] S. Tan, C. Wang, C.-W. Shu and J. Ning, *Efficient implementation of high order inverse Lax-Wendroff boundary treatment for conservation laws*, Journal of Computational Physics, v231 (2012), pp.2510-2527.

[6] F. Vilar and C.-W. Shu, *Development and stability analysis of the inverse Lax-Wendroff boundary treatment for central compact schemes*, ESAIM: Mathematical Modelling and Numerical Analysis (M^2AN), v49 (2015), pp.39-67.

[7] T. Li, C.-W. Shu and M. Zhang, *Stability analysis of the inverse Lax-Wendroff boundary treatment for high order upwind-biased finite difference schemes*, Journal of Computational and Applied Mathematics, v299 (2016), pp.140-158.

[8] S. Ding, C.-W. Shu and M. Zhang, *On the conservation of finite difference WENO schemes in non-rectangular domains using the inverse Lax-Wendroff boundary treatments*, Journal of Computational Physics, v415 (2020), 109516.

[9] J. Lu, C.-W. Shu, S. Tan and M. Zhang, *An inverse Lax-Wendroff procedure for hyperbolic conservation laws with changing wind direction on the boundary*, submitted to Journal of Computational Physics.

Compressible inviscid flows involving complex moving geometries

We extend the high order accurate numerical boundary condition based on finite difference methods to simulations of compressible inviscid flows involving complex moving geometries.

- For problems in such geometries, it is difficult to use body-fitted meshes which conform to the moving geometry.
- Instead, methods based on fixed Cartesian meshes have been successfully developed. For example, the immersed boundary (IB) method introduced by Peskin (JCP 1972) is widely used. One of the challenges of the IB method is the representation of the moving objects which cut through the grid lines in an arbitrary fashion.

- To solve compressible inviscid flows in complex moving geometries, most methods in the literature are based on finite volume schemes. The challenge mainly comes from the so-called “small-cell” problem. Namely, one obtains irregular cut cells near the boundary, which may be orders of magnitude smaller than the regular grid cells, leading to a severe time step restriction.
- In terms of accuracy, most finite volume schemes in the literature are at most second order. In particular, the errors at the boundaries sometimes often fall short of second order.
- Our inverse Lax-Wendroff procedure can be extended to such situations with moving geometries. The only change is to obtain relationships between the temporal and spatial derivatives via the PDE in moving Lagrangian framework.

Example 7. We consider a gas confined between two rigid walls. The right wall is fixed at $x_r = 1.0$ while the left wall is moving. We assume the left wall is positioned at $x_l(t) = 0.5(1 - t)$. The initial conditions are

$$\begin{aligned} \rho(x,0) &= 1 + 0.2\cos\left[2\pi\left(x - 0.5\right)\right], \\ u(x,0) &= x - 1, \\ p(x,0) &= \rho(x,0)^\gamma, \end{aligned}$$

such that the initial entropy $s(x,0) = 1$. As long as the solution stays smooth, we have isentropic flow, i.e., $s(x,t) = 1$. Thus the numerical value of the entropy can be used for the analysis of convergence.

Table 6: Entropy errors and convergence rates of Example 7

h	$x_l(t) = 0.5(1 - \sin t)$			
	L^1 error	order	L^∞ error	order
1/40	7.26E-07		1.32E-06	
1/80	1.15E-08	5.98	2.82E-08	5.55
1/160	3.43E-10	5.07	6.19E-10	5.51
1/320	9.90E-12	5.11	2.49E-11	4.64

Example 8. This is a 1D problem involving shocks and rarefaction waves. A piston with width $10h$ is initially centered at $x = -5h$ inside a shock tube. Here h is the mesh size. The piston instantaneously moves with a constant velocity $u_p = 2$ into an initially quiescent fluid with $\rho = 1$ and $p = 5/7$. This problem is equivalent to two independent Riemann problems and thus the exact solution can be obtained. A shock forms ahead of the piston and a rarefaction wave forms in the rear.

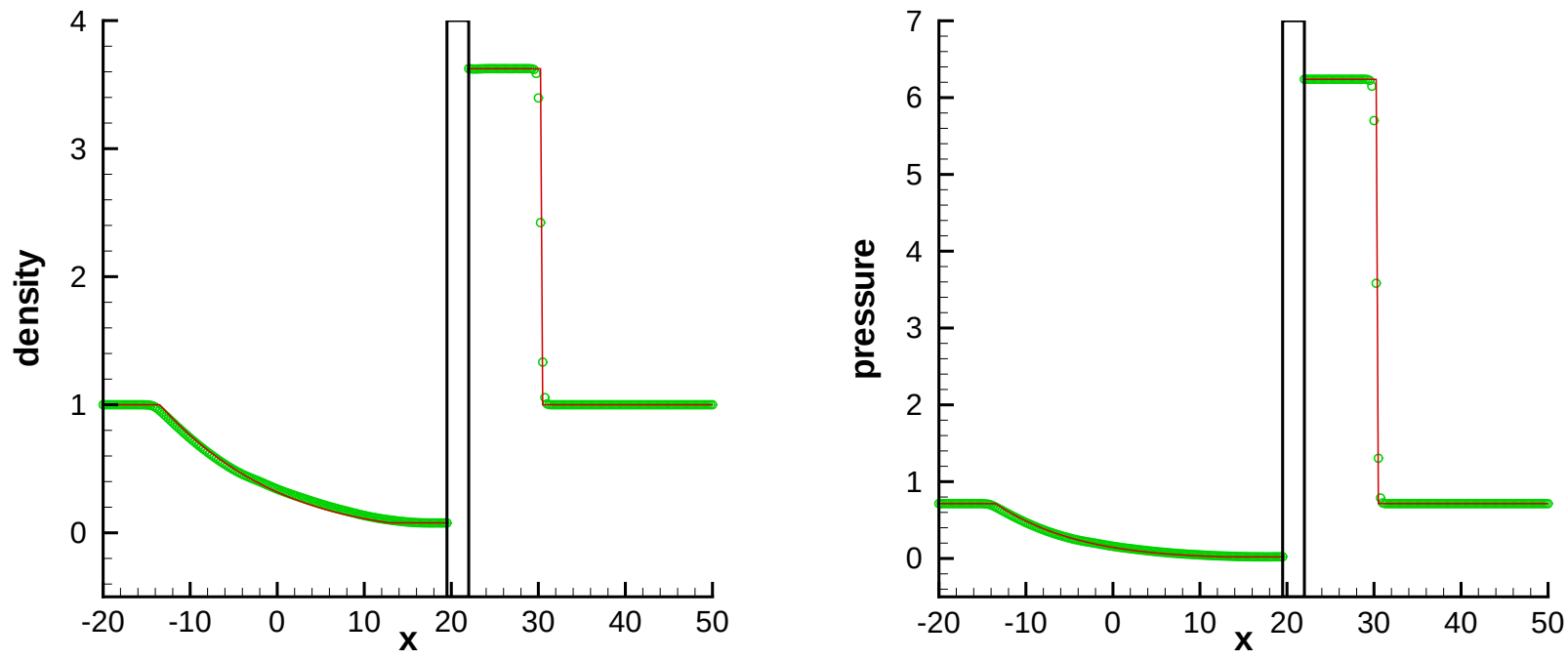

(a) Density (b) Pressure

Figure 11: Density and pressure profiles of Example 8. The piston is represented by the rectangle. Solid lines: exact solutions; Symbols: numerical solutions with $h = 0.25$.

Example 9. The last example shows that our high order method can also treat a rigid body whose motion is induced by the fluid. We test the so-called cylinder lift-off problem. In this problem, a rigid cylinder initially resting on the floor of a 2D channel is driven and lifted by a strong shock. The computational domain is $[0, 1] \times [0, 0.2]$. A rigid cylinder with radius 0.05 and density 10.77 is initially centered at $(0.15, 0.05)$. A Mach 3 shock starts at $x = 0.08$ moving towards the cylinder. The density and pressure of the resting gas are $\rho = 1.4$ and $p = 1.0$ respectively. The top and bottom of the domain are rigid walls. The left boundary is set to the post-shock state and the right boundary is supersonic outflow.

Table 7: Center of the cylinder of Example 9.

h	$t = 0.1641$		$t = 0.30085$	
	x-coordinate	y-coordinate	x-coordinate	y-coordinate
1/160	3.7058E-01	8.1140E-02	6.7178E-01	1.3759E-01
1/320	3.6153E-01	8.3219E-02	6.4959E-01	1.4444E-01
1/640	3.5706E-01	8.3680E-02	6.3895E-01	1.4517E-01
1/1280	3.5539E-01	8.4133E-02	6.3550E-01	1.4607E-01
1/2560	3.5461E-01	8.4258E-02	6.3362E-01	1.4638E-01

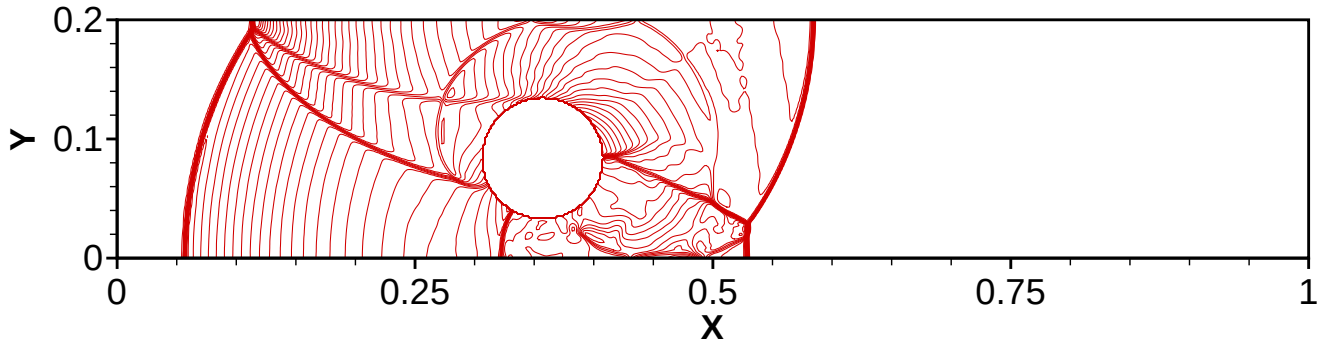

(a) $h = 1/640$

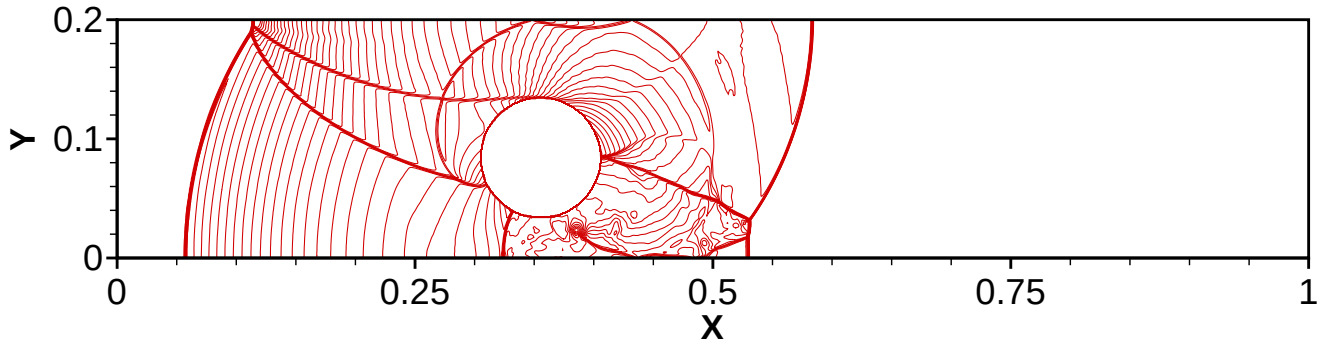

(b) $h = 1/1280$

Figure 12: Pressure contours at $t = 0.1641$. 53 contours from 2 to 28. $t = 0.1641$.

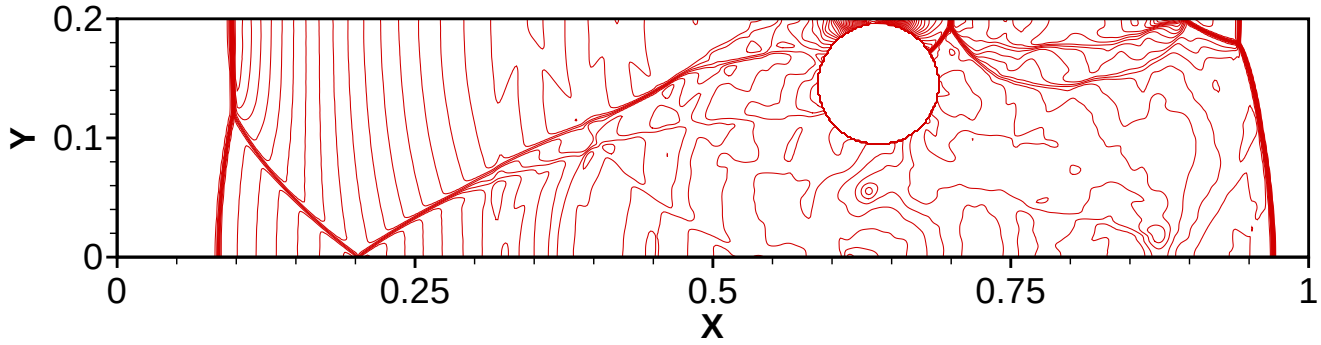

(a) $h = 1/640$

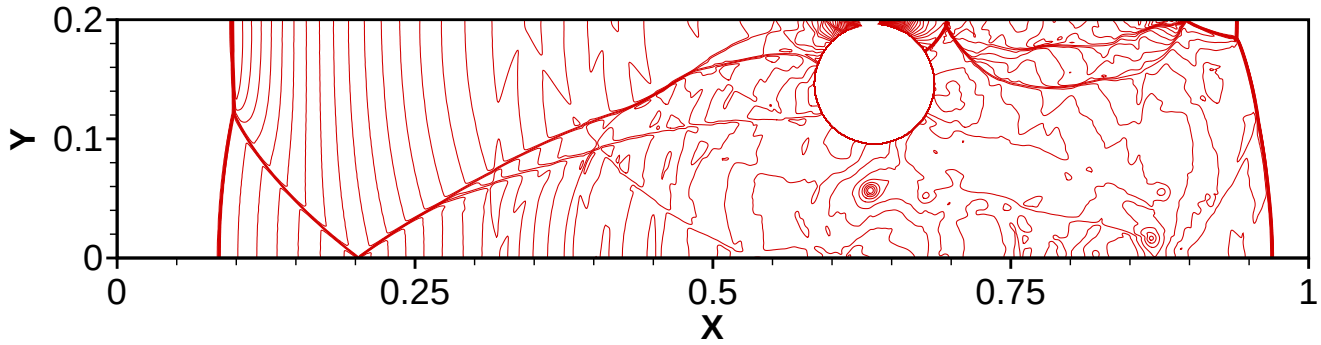

(b) $h = 1/1280$

Figure 13: Pressure contours at $t = 0.30085$. 53 contours from 2 to 28. $t = 0.30085$.

Reference:

[10] S. Tan and C.-W. Shu, *A high order moving boundary treatment for compressible inviscid flows*, Journal of Computational Physics, v230 (2011), pp.6023-6036.

[11] S. Tan and C.-W. Shu, *Inverse Lax-Wendroff procedure for numerical boundary conditions of hyperbolic equations: survey and new developments*, in “Advances in Applied Mathematics, Modeling and Computational Science”, R. Melnik and I. Kotsireas, Editors, Fields Institute Communications 66, Springer, New York, 2013, pp.41-63.

Convection-diffusion equations

The extension to convection-diffusion equations is non-trivial, since totally different boundary treatments are needed for the diffusion-dominated and the convection-dominated regimes.

We look at the simple example of heat equation:

$$u_t = u_{xx}, \qquad 0 < x < \infty$$

with boundary condition

$$u(0,t) = g(t).$$

If we perform a Taylor expansion at $x = 0$

$$u_j = u(0,t) + u_x(0,t)x_j + \frac{1}{2}u_{xx}(0,t)x_j^2 + \cdots$$

then the inverse Lax-Wendroff procedure can only determine the even order derivatives:

$$u(0,t) = g(t), \quad u_{xx}(0,t) = g'(t), \cdots$$

and the odd derivatives must be obtained by extrapolation.

Stability of such inverse Lax-Wendroff procedure, when the relative location of the boundary and the closest grid point is arbitrary, and for both Dirichlet and Neumann boundary conditions, is systematically analyzed in (Li, Shu and Zhang, JSC 2017),

Now, suppose we have a convection-diffusion equation

$$u_t + au_x = \varepsilon u_{xx}, \qquad 0 < x < \infty$$

with boundary condition

$$u(0,t) = g(t).$$

There are two ways of applying the inverse Lax-Wendroff procedure to obtain the first two spatial derivatives:

1. The first approach is to use extrapolation to obtain the second derivative $u_{xx}(0,t) = u_{xx}^{ext}$, and then use the inverse Lax-Wendroff procedure to obtain the first derivative

$$u_x(x,0) = \frac{1}{a}\left(g'(t) - \varepsilon u_{xx}^{ext}\right)$$

   The remaining derivatives can be obtained similarly. This is the approach for the purely convection equation ($\varepsilon = 0$), hence it is expected to work well for convection-dominated situation.

2. The second approach is to use extrapolation to obtain the first derivative $u_x(0,t) = u_x^{ext}$, and then use the inverse Lax-Wendroff procedure to obtain the second derivative

$$u_{xx}(x,0) = \frac{1}{\varepsilon}\left(g'(t) + a u_x^{ext}\right)$$

The remaining derivatives can be obtained similarly. This is the approach for the purely diffusion equation ($a = 0$), hence it is expected to work well for diffusion-dominated situation.

In (Lu, Fang, Tan, Shu and Zhang, JCP 2016), we have designed a careful combination of the boundary treatments for the two regimes and obtained a stable and accurate boundary condition for general convection-diffusion equations, which worked well for various test cases including compressible Navier-Stokes equations.

Reference:

[12] J. Lu, J. Fang, S. Tan, C.-W. Shu and M. Zhang, *Inverse Lax-Wendroff procedure for numerical boundary conditions of convection-diffusion equations*, Journal of Computational Physics, v317 (2016), pp.276-300.

[13] T. Li, C.-W. Shu and M. Zhang, *Stability analysis of the inverse Lax-Wendroff boundary treatment for high order central difference schemes for diffusion equations*, Journal of Scientific Computing, v70 (2017), pp.576-607.

Concluding remarks

- We have demonstrated an inverse Lax-Wendroff procedure for boundary treatment, which yields stable discretization with the same CFL number as the inner scheme and allows us to compute problems on arbitrary domains using Cartesian meshes.
- The technique can be applied to inviscid and viscous flows with complex moving geometries, yielding stable and high order accurate solutions.
- Future work would involve a generalization of this technique to other schemes such as the discontinuous Galerkin method, and to problems with deformable structures and interface problems.

The End

THANK YOU!